MITSUBISHI ELECTRIC RESEARCH LABORATORIES
http://www.merl.com

# A Channel Model for Ultrawideband Indoor Communication

Foerster, J.; Pendergrass, M.

TR2003-73 November 2003

**Abstract**

This paper describes the wireless channel model that the IEEE 802.15.3a standardization group has developed for the evaluation of ultrawideband communications systems. We discuss the measurements that form the basis of this model. These measurements establish important differences between UWB channels and narrowband wireless channels, especially with respect to fading statistics and time-of-arrival of multipath components. The different propagation conditions impact system design, like Rake receiver performance.

**Publication History:**

1. First printing, TR-2003-73, November 2003

# A Channel Model for Ultrawideband Indoor Communication

Jeffrey R. Foerster, *Member, IEEE* , Marcus Pendergrass, *Member, IEEE*
and Andreas F. Molisch, *Senior Member, IEEE*

J. Foerster is with Intel Corporation, Hillsboro, OR, USA (jeffrey.r.foerster@intel.com)
Marcus Pendergrass is with Time Domain Corp. Huntsville, AL, USA
and Dept. of Mathematics, University of Alabama at Huntsville, Huntsville, Alabama, USA
(marcus.pendergrass@timedomain.com)
A. F. Molisch is with Mitsubishi Electric Research Labs, Cambridge, MA, USA
and Dept. of Electroscience, Lund University, Lund, Sweden (Andreas.Molisch@ieee.org)

**Abstract:** This paper describes the wireless channel model that the IEEE 802.15.3a standardization group has developed for the evaluation of ultrawideband communications systems. We discuss the measurements that form the basis of this model. These measurements establish important differences between UWB channels and narrowband wireless channels, especially with respect to fading statistics and time-of-arrival of multipath components. The different propagation conditions impact system design, like Rake receiver performance.

## 1. Introduction

In recent years, ultrawideband (UWB) communications has received great interest from both the research community and industry. The potential strength of the UWB radio technique lies in its use of extremely wide transmission bandwidths, which results in desirable capabilities including accurate position location and ranging, lack of significant fading, high multiple access capability, covert communications, and possible easier material penetration. In February 2001, the American FCC (Federal Communications Commission) issued a report and order that allows the transmission of UWB signals if certain power restrictions are fulfilled. Other countries, especially Japan and Europe, are expected to issue similar rulings in the near future.

A main application for these system are high-data rate systems for short distances, as are, e.g., intended for wireless linking of home entertainment components (VCR, TV, Set-top boxes, etc.). A standard for such systems is currently being developed by the standardization group IEEE 802.15.3a. The target bitrates of this new standard are data rates of up to 110 Mbit/s at 10m distance, 200Mbit/s at 4m distance, and higher data rates at smaller distances. More than 20 organizations have submitted proposals for this standard. A fair evaluation of those proposals must use a common channel model. However, existing standard models (like the COST 259, ITU-R, or IEEE 802.11 models) cannot be used, because they are only intended to model *narrowband* channels. For this reason, IEEE 802.15.3a formed a subgroup for the development of a standard UWB channel model; its proposal was accepted by the full standardization group. In this paper, we describe this channel model, and the new effects arising in wireless propagation channels due to the ultrawide bandwidth.

The remainder of the paper is organized the following way: in Sec. 2, we discuss the measurements that form the basis of the model. Section 3 then describes the detailed specifications. A discussion on the implications of the model for system design and simulation conclude the paper.

## 2. Measurements

The measurement and modeling of UWB channels is a fairly recent field. The 802.15 channel model is based on some of the measurement campaigns published in the open literature see, e.g., [5], [6], [7], as well as on measurement campaigns performed explicitly for the standard. These new campaigns were carried out by various standardization participants, and their data were used to assess the goodness of fit of various proposed channel models, as well as to calibrate their parameters.

There are two basic techniques for UWB channel sounding.

1. In time-domain techniques, the channel is excited by a short pulse, and the receiver records the impulse response directly, by sampling the received waveform. The advantage of this technique is that it gives the waveform directly in the time domain, and time variations of the channels can be easily measured. The drawback lies in the problems of producing ultra-short pulses, and the fact that a

nonideal transmit pulse distorts the observed impulse response. Applying a devonvolution of the transmit pulse from the received signal often leads to numerical problems.

2. In swept-frequency measurements, a chirp (time-varying sinusoid) is used to excite the channel, so that the received signal is an approximation of the transfer function. In most practical cases, a network analyzer is used as transceiver, since these devices are well-calibrated, and readily available in most laboratories. A further advantage of this technique is that a "back-to-back calibration" can be done quite easily. A drawback is that time variations of the channels cannot be easily recorded. However, this was not a major requirement for the modeling in 802.15.

All the measurement environments were indoor, as this is the target application for 802.15.3a devices. Different types of indoor environments were analyzed, including residential (homes, apartments), and office environments. The building materials and geometrical layouts are quite different in those cases, and result in distinct channel characteristics. This is due mostly to the higher proportion of metal construction materials found in office buildings as compared to residential buildings. In addition to these environment types, most contributors distinguished between line-of-sight channels, in which there is an unobstructed path from transmitter to receiver, from non-line-of-sight channels.

Also, the choice of measurement points were different: some campaigns used regular grids in order to isolate small-scale from large-scale fading effects, while other campaigns used only random placement of measurement points on a large scale.

The amount of measurement results was actually too large for an efficient application to the modeling process. The 802.15.3a channel modeling subgroup thus selected a subset of measurements that was to be used for the actual parameterization of measurements, as well as the goodness-of-fit test of those models. Part of these measurements has been made publicly available at [6].

Since it may be difficult for a single model to reflect all of the possible channel environments and characteristics, the group chose to try and match the following primary characteristics of the multipath channel:

- RMS delay spread
- Power delay profile
- Number of multipath components (defined as the number of multipath arrivals that are within 10 dB of the peak multipath arrival)

# 3. The IEEE 802.15.3a standard model

The large bandwidth of UWB channels can give rise to new effects compared to "conventional" wireless channel modeling. For example, only few multipath components overlap within each resolvable delay bin (resolvable runlength is 3cm), so that the central limit theorem is no longer applicable, and the amplitude fading statistics are no longer Rayleigh. Also, there can be delay bins into which no MPCs fall, and thus are empty. It then becomes necessary to characterize the likelihood that this happens, and that an empty bin is followed by a full one – in other words, to obtain the time-of-arrival statistics.
For the time-of-arrival statistics, the model uses a Saleh-Valenzuela (S-V) approach [2], as the channel measurements showed multipaths arriving in clusters. This is partly a result of the very fine resolution that ultra-wideband waveforms provide. For example, multipath results from reflections off walls, ceilings, furniture, people, and other objects that may be present within a room. Since UWB waveforms can be up to 7.5 GHz wide, for example, paths separated by more than about 133 ps (equivalent to 4cm pathlength difference) can be individually resolved at the receiver. Thus, different parts of the same furniture piece can give rise to several multipath components, all of which would be part of one cluster.

The SV model thus distinguishes between "cluster arrival rates" and "ray arrival rates". The first cluster starts by definition at time t=0, and the following rays are a arriving with a rate given by a Poisson process with rate λ. The power of those rays decays exponentially with increasing delay from the first ray. The "cluster arrival rate", which is smaller than the ray arrival rate, in turn determines when the next cluster has its origin. The rays within that cluster are again a Poisson process with rate λ.

Mathematically, the impulse response is described as

$$h_i(t) = X_i \sum_{l=0}^{L} \sum_{k=0}^{K} \alpha_{k,l}^i \delta(t - T_l^i - \tau_{k,l}^i)$$

where

- $\{\alpha_{k,l}^i\}$ are the multipath gain coefficients,
- $\{T_l^i\}$ is the delay of the $l^{th}$ cluster,
- $\{\tau_{k,l}^i\}$ is the delay of the $k^{th}$ multipath component relative to the $l^{th}$ cluster arrival time ($T_l^i$),
- $\{X_i\}$ represents the log-normal shadowing, and $i$ refers to the $i^{th}$ realization.

Defining

- $T_l$ = the arrival time of the first path of the *l*-th cluster;
- $\tau_{k,l}$ = the delay of the *k*-the path within the *l*-th cluster relative to the first path arrival time, $T_l$;
- $\Lambda$= cluster arrival rate;
- $\lambda$=ray arrival rate, i.e., the arrival rate of path within each cluster.

By definition, $\tau_{0,l} = 0$. The distribution of cluster arrival time and the ray arrival time are given by

$$p\left(T_l \left| T_{l-1}\right.\right) = \Lambda \exp\left[-\Lambda\left(T_l - T_{l-1}\right)\right], \quad l > 0$$
$$p\left(\tau_{k,l}\left|\tau_{(k-1),l}\right.\right) = \lambda \exp\left[-\lambda\left(\tau_{k,l} - \tau_{(k-1),l}\right)\right], \quad k > 0$$

The channel coefficients are defined as a product of small-scale and large-scale fading coefficients, i.e.,

$$\alpha_{k,l} = p_{k,l}\xi_l\beta_{k,l},$$

The amplitude statistics of the measurements were found to best fit the log-normal distribution rather than the Rayleigh.that was used in the original SV model. In addition, the large-scale fading is also lognormally distributed.

$$20\log10(\xi_l\beta_{k,l}) \propto \text{Normal}(\mu_{k,l}, \sigma_1^2 + \sigma_2^2),$$

or

$$\left|\xi_l\beta_{k,l}\right| = 10^{(\mu_{k,l}+n_1+n_2)/20}$$

where

$$n_1 \propto \text{Normal}(0, \sigma_1^2)$$

and

$$n_2 \propto \text{Normal}(0, \sigma_2^2)$$

are independent and correspond to the fading on each cluster and ray, respectively.

The behavior of the (averaged) power delay profile is

$$E\left[\left|\xi_l\beta_{k,l}\right|^2\right] = \Omega_0 e^{-T_l/\Gamma} e^{-\tau_{k,l}/\gamma},$$

which reflects the exponential decay of each cluster, as well as the decay of the total cluster power with delay.

$p_{k,l}$ is equiprobable +/-1 to account for signal inversion due to reflections. The $\mu_{k,l}$ is given by

$$\mu_{k,l} = \frac{10\ln(\Omega_0) - 10T_l/\Gamma - 10\tau_{k,l}/\gamma}{\ln(10)} - \frac{(\sigma_1^2 + \sigma_2^2)\ln(10)}{20}$$

In the above equations, $\xi_l$ reflects the fading associated with the $l^{th}$ cluster, and $\beta_{k,l}$ corresponds to the fading associated with the $k^{th}$ ray of the $l^{th}$ cluster. Note that, a complex tap model was not adopted here. The complex baseband model is a natural fit for narrowband systems to capture channel behavior independently of carrier frequency, but this motivation breaks down for UWB systems where a real-valued simulation at RF may be more natural.

Finally, since the log-normal shadowing of the total multipath energy is captured by the term, $X_i$, the total energy contained in the terms $\{\alpha_{k,l}^i\}$ is normalized to unity for each realization. This shadowing term is characterized by the following:

$$20\log10(X_i) \propto \text{Normal}(0, \sigma_x^2).$$

While the above model is quite general, it still contains a considerable number of simplifications. First., we assume that the cluster and ray arrival rates are delay-invariant. However, this is not necessarily the case. Especially for very small delays, arrival rates are considerably smaller than for large delays. This is intuitively clear, as there are only few physically possible propagation paths from transmitter to receiver that have a small excess delay, while that number increases with delay. This effect has also been shown in measurements. However, in the interest of simplicity, the 802.15.3a model does not reflect that effect.

The model also assumes that the variance of the lognormal fading is independent of the delay. Again, this is not the most general case. An argument similar to the above shows that the relative variance should be smaller for small delays than for large delays, a fact that was confirmed, e.g., in [5]. We have also compared the amplitude distribution to the Nakagami distribution and found that both the log-normal and Nakagami distributions can fit the data equally well.

The proposed model parameters were designed to fit measurement results described in Sec. 2. Four different measurement environments were defined, namely CM1, CM2, CM3, and CM4. CM1 describes a LOS (line-of-sight) scenario with a separation between transmitter and receiver of less than 4m. CM2 describes the same range, but for a non-LOS situation. CM3 describes a non-LOS scenario for distances between TX and RX 4-10m. Scenario 4 finally describes an environment with strong delay dispersion, resulting in a delay spread of 25ns.

Note that, when using the model, the total average received power of the multipath realizations is typically normalized to unity in order to provide a fair comparison with other wideband and narrowband systems. The channel characteristics and corresponding parameter matching results in Table 1 correspond to a time resolution of 167 psec, although the output of the model described in the appendix yields continuous time samples (i.e., based upon an infinite bandwidth). How this model matches measurements with bandwidths greater than 6 GHz is unknown due to the lack of measurement data at this bandwidth.

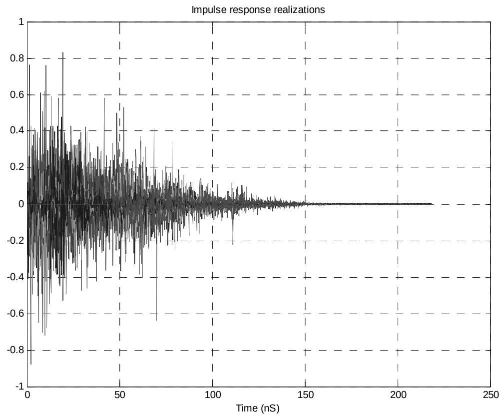


**Figure 1 100 impulse responses based on CM3.**

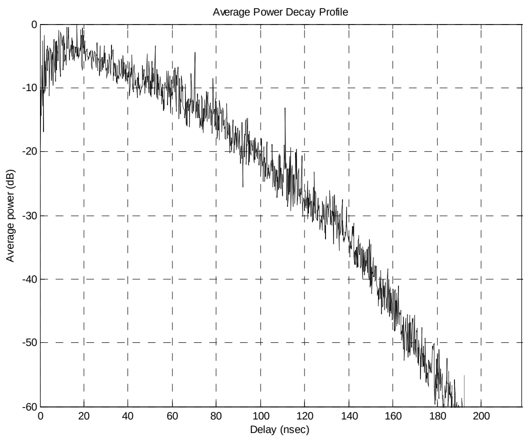


**Figure 2 Average power delay profile for CM 3**

Figures 1 and 2,show some important characteristics of characteristics of channels obtained from this model. The delay spread is at least several nanoseconds, leading to considerable inter-symbol interference (ISI) if UWB pulses are closely spaced in time. This necessitates some form of countermeasure. On the other hand, this also implies a high degree of available diversity for the receiver.

# 4. Summary and conclusion

The structure of the channel model has a strong influence on the system performance assessment. For example, the long delay spread (several nanoseconds) can have both positive and negative implications. It is good in the sense that the multipath arrivals will undergo less amplitude fluctuations (fading) since there will be fewer reflections that cause destructive/constructive interference within the resolution time of the received impulse. On the other hand, the average total received energy is distributed between a number of multipath arrivals. In order to take advantage of that energy, unique systems and receivers need to be designed with multipath energy capture in mind.

Summarizing, the 802.15 standard model was an important step for the understanding of UWB channels, and was established in time to be useful for the selection process of the new standard for UWB high-data rate communications. But it is not a universal stochastic model of the wireless propagation channel, and a lot of work will have to be spent by the channel modeling community before our understanding of UWB channels is complete.

**Acknowledgments:** The authors are indebted to a number of significant contributions that were submitted to the IEEE 802.15.3a study group, which helped to form this channel model and provide a means of evaluating UWB physical layers for next generation, high-rate WPANs. The individual contributors are too many to name, but are listed in [4], and the authors would like to acknowledge their contributions to art of UWB channel modeling.

## References

[1] IEEE 802.11-97/96, Naftali Chayat, September 1997.
[2] A. Saleh and R. Valenzuela, “A Statistical Model for Indoor Multipath Propagation,” IEEE JSAC, Vol. SAC-5, No. 2, Feb. 1987, pp. 128-137.
[3] H. Hashemi, “Impulse Response Modeling of Indoor Radio Propagation Channels,” IEEE JSAC, Vol. 11, No. 7, Sept. 1993, pp. 967-978.
[4] J. Foerster (editor), “Channel Modeling Sub-committee Report Final,” IEEE802.15-02/490 (see http://ieee802.org/15/)
[5] D. Cassioli, M. Z. Win, and A. F. Molisch, „The Ultra-Wide Bandwidth Indoor Channel - From Statistical Model to Simulations“, IEEE JSAC, 20, 1247-1257 (2002).
[6] http://ultra.usc.edu/New_Site/database.html

**Table 1**: Multipath channel target characteristics and model parameters.

| **Target Channel Characteristics**[5] | **CM** | **CM 2** | **CM 3** | **CM 4** |
|---|---|---|---|---|
| $\tau_m$ [ns] (Mean excess delay) | 5.05 | 10.38 | 14.18 | |
| $\tau_{rms}$ [ns] (rms delay spread) | 5.28 | 8.03 | 14.28 | 25 |
| $NP_{10dB}$ (number of paths within 10 dB of the strongest path) | | | 35 | |
| NP (85%) (number of paths that capture 85% of channel energy) | 24 | 36.1 | 61.54 | |
| **Model Parameters** | | | | |
| $\Lambda$ [1/nsec] (cluster arrival rate) | 0.0233 | 0.4 | 0.0667 | 0.0667 |
| $\lambda$ [1/nsec] (ray arrival rate) | 2.5 | 0.5 | 2.1 | 2.1 |
| $\Gamma$ (cluster decay factor) | 7.1 | 5.5 | 14.00 | 24.00 |
| $\gamma$ (ray decay factor) | 4.3 | 6.7 | 7.9 | 12 |
| $\sigma_1$ [dB] (stand. dev. of cluster lognormal fading term in dB) | 3.3941 | 3.3941 | 3.3941 | 3.3941 |
| $\sigma_2$ [dB] (stand. dev. of ray lognormal fading term in dB) | 3.3941 | 3.3941 | 3.3941 | 3.3941 |
| $\sigma_x$ [dB] (stand. dev. of lognormal fading term for total multipath realizations in dB) | 3 | 3 | 3 | 3 |
| **Model Characteristics**[5] | | | | |
| $\tau_m$ | 5.0 | 9.9 | 15.9 | 30.1 |
| $\tau_{rms}$ | 5 | 8 | 15 | 25 |
| $NP_{10dB}$ | 12.5 | 15.3 | 24.9 | 41.2 |
| NP (85%) | 20.8 | 33.9 | 64.7 | 123.3 |
| Channel energy mean [dB] | -0.4 | -0.5 | 0.0 | 0.3 |
| Channel energy std dev. [dB] | 2.9 | 3.1 | 3.1 | 2.7 |
| | | | | |

.